Available online at www.sciencedirect.com
SCIENCE DIRECT®
Journal of Structural Biology 146 (2004) 334–343
Journal of Structural Biology
www.elsevier.com/locate/yjsbi

AFM of biological material embedded in epoxy resin

Nadezda Matsko and Martin Mueller*

Electron Microscopy, Institut fuer Angewandte Physik, ETH-Hoenggerberg, CH-8093, Zuerich, Switzerland

Received 19 October 2003, and in revised form 21 January 2004

Abstract

We present a simple method to extract morphological details from the block face of epoxy embedded biopolymers by AFM. It is shown that topographical contrast and the identification of small structural details critically depend on the procedure of sample preparation before embedding (chemical fixation or high-pressure freezing and freeze-substitution) and on the hardness of the embedding epoxy resin. Ethanol treatment of the block face of the sample after microtomy elutes non-cross-linked polymer chains and makes the smallest details of the embedded biomaterial amenable to detection. AFM (height and phase contrast) examination of the block face of accordingly prepared cells of *Caenorhabditis elegans* provides data that are comparable to TEM.

Keywords: Atomic force microscopy; Epoxy resin; Freeze-substitution; High-pressure freezing; Microtomy; Transmission electron microscopy

1. Introduction

The scanning probe techniques in life sciences all allow imaging at the level of individual molecules. Furthermore, molecules can be addressed individually and experiments performed, setting these techniques apart from any other microscopy technique. So far, these methods have been limited to probe essentially planar interfaces, being either the plasma membrane or isolated macromolecules and macromolecular assemblies. We have now made the interior of the cells and tissues accessible to atomic force microscopy (AFM), using a well established technique to prepare tissue and cell samples for the transmission electron microscope (TEM).

Our current understanding of the cellular ultrastructure is largely derived from the analysis of thin sections of resin embedded biological material by transmission electron microscopy.

Basic considerations of the process of ultrathin sectioning (Jesior, 1985, 1986) indicate that most section artifacts (compression, chatter, and knife marks) are, with the exception of the knife marks, mainly expressed in the ultrathin section and not in the block face, which can be extremely smooth. The use of the block face for studies of the ultrastructure of cells and tissue by AFM appears, therefore, promising, since the resolution with AFM techniques is best on samples with small (or limited) corrugation of the surface as the effects of the tip geometry and other artifacts are minimized (Abraham et al., 1988; Akamine et al., 1990). Also on surfaces with local variations of mechanical properties such as polymers and biological samples, the AFM phase images provide the best contrast of fine morphological and nanostructural features (Fasolka et al., 2001; Haugstad and Jones, 1999).

Here we report the successful structural analysis of the blockface of resin embedded and sectioned biological material by atomic force microscopy. We show that the quality of the embedding resin and its interaction with the biological material is crucial for adequate height (topography) and phase (local variations of mechanical properties) contrast. Note that the production of flat surfaces for AFM investigation by ultra-microtomy at room or low temperature has found wide application in polymer sciences (Magonov and Reneker, 1997). However, earlier attempts to characterize the ultrastructure of biological material in this way did not provide convincing results (Melling et al., 2001; Nag et al., 1999; Yamamoto and Tashiro, 1994).

The proposed approach to study the complexity of the ultrastructure of cells and tissues by AFM essentially

* Corresponding author. Fax: +41-1-632-1103.
E-mail address: mmueller@iap.phys.ethz.ch (M. Mueller).

1047-8477/$ - see front matter © 2004 Elsevier Inc. All rights reserved.
doi:10.1016/j.jsb.2004.01.010

depends on experience from the corresponding TEM techniques to prepare biological specimens.

The appearance of the ultrastructural elements in TEM varies with the applied protocol (buffers, chemical fixation and dehydration or cryofixation followed by freeze-substitution, type of embedding resin, etc.). Apart from the quality of the structural preservation by different fixation protocols, the interaction with the embedding resin may vary in addition and will finally result in a different copolymerization of biological and resin macromolecules (Causton, 1985).

It is generally accepted, that cryoimmobilisation based specimen procedures for electron microscopy preserve best the biological ultrastructure. Very high cooling rates, necessary to prevent formation and growth of ice crystals, guarantee a high time resolution for dynamic cellular events, i.e., a rapid arrest of all physiological processes in contrast to chemical fixation which is relatively slow and preserves the ultra-structure as a function of the response to the diffusion of the fixatives and the dehydrating agents (osmotic effects, shrinkage, loss, and redistribution of ions). Aqueous samples up to a thickness of 150–200 μm can be adequately frozen by high pressure freezing (Dahl and Staehelin, 1989; Moor and Hochli, 1968; Moor, 1987; Mueller and Moor, 1984; Studer et al., 1992). Purely physical follow-up procedures such as cryo-sectioning and freeze-fracturing, can serve as references by which possible structural effects of the most frequently used freeze-substitution method may be characterized. Freeze-substitution is a hybrid technique that combines improved structural preservation with the ease of sectioning at room temperature. During freeze-substitution, the frozen water is dissolved at low temperatures in an organic solvent (mainly acetone) in which OsO_4 (2%) and/or uranyl-ions may be present as fixing agents (Van Harreveld and Crowell, 1964). Chemical stabilization and dehydration, thus, are performed under conditions in which the biological structures are stabilized by the cold. This results in an improved preservation of the ultrastructure at least with respect to the relative dimensions, since osmotic effects become negligible (Menco, 1984, 1995). After freeze-substitution, the biological structures appear to be less rigidly stabilized than after chemical fixation with aldehydes and OsO_4, followed by dehydration in graded series of organic solvents. This may result in a different interaction of the biological material with the embedding chemistry.

Resins suitable for electron microscopy generally are of amorphous nature. Epoxy resins are the most frequently used amorphous polymers in electron microscopy. For embedding, a stock solution containing one or two different epoxy resins and plasticizer is mixed with a crosslinker (hardener) and an accelerator. This mixture is used to impregnate the biological sample in steps of decreasing dilution in an organic solvent. After impregnation with 100% plastic, the polymerization is started and catalyzed at 60 °C (Luft, 1961; Mollenhauer, 1964).

The role of embedding for electron microscopy is to transfer the soft biological material into a solid state, in which the structural details remain preserved and which is hard enough to facilitate the fabrication of the required ultrathin sections. The stability of the plastic and its interaction with the biological material must in addition resist the impact of the electron microscopes (vacuum, electron bombardement). Harder epoxy resins generally permit thinner sections and show less mass loss under the electron beam. On the other hand, improved structural preservation is reported with softer resin formulations (Mollenhauer and Drolesky, 1997) i.e., reduced crosslink density (Causton, 1985).

2. Materials and methods

2.1. High-pressure freezing, freeze-substitution, and embedding

Nematodes (Caenorhabditis elegans), a kind gift of Prof. M. Gotti, ETH Zürich, were high pressure frozen in cellulose capillaries as described earlier (Hohenberg et al., 1994) using a HPM 010 apparatus (Bal-Tec, Lichtenstein), and subsequently freeze-substituted in acetone containing 2% of OsO_4, at −90 °C for 8 h, at −60 °C for 8 h, at −30 °C for 8 h, and at 0 °C for 1 h. After warming up to room temperature, the samples were embedded in resin mixtures with different hardness according to Table 1. Infiltration was performed stepwise (33% resin in water free acetone for 4 h, 66% resin in acetone for 4 h, and 100% resin overnight in a desiccator, evacuated with a membrane pump to 10 mbar to maintain dry conditions). Impregnation steps with diluted (33 and 66%) resin were performed with and without the addition of the accelerator component (according to Table 1). All samples were polymerized at 60 °C for 72 h. Blockfaces for AFM analysis were produced within 1 day after polymerization.

Table 1
Composition of epoxy resin mixtures (Hayat, 2000)

Ingredients (g)	Hard	Rigid	Soft
Epon 812	42.7	31.7	31.7
Durcupan ACM	5.6	17.9	17.9
DDSA (dodecenyl succinic anhydride)	57.6	52.6	52.6
DP (dibutylphtalate)	—	2	4
Total	105.9	104.3	106.3

Note. To accomplish polymerization, 10 drops of the accelerator DMP-30 (2,4,6-tris(dimethylaminomethyl) phenol) were added to 10 g of the mixture.

2.2. Ultrathin sections and block face preparation

The resin embedded specimens were mounted in special holders which at the same time fit the microtome and are suitable for the examination of the block face by AFM. Ultrathin sections were obtained using a Leica Ultracut E microtome (Leica, Austria) equipped with a diamond knife (Diatome, Switzerland). Sections for TEM analysis were collected on carbon coated formvar supports, stained with uranyl acetate and lead citrate (Reynolds, 1963) and examined in a Zeiss EM 912 Omega (LEO, BRD) electron microscope equipped with a ProScan slow scan CCD camera.

The block faces of some specimens were treated with pure ethanol for varying time prior to AFM examination.

2.3. Atomic force microscopy

AFM images were collected in tapping mode using Digital Instruments NanoScope III equipped with a J scanner (scanning range 150 μm) and silicone nitride cantilevers with natural frequencies in the 300 kHz range (force constant 10 N/m, tip radius 10 nm (NT-MDT, Russia)). All images were made with A_o (free-air probe oscillation amplitude) set to 2 V which after landing was increased to 10–15 V. A_{sp} (sample contact amplitude) was set to 1.0–0.9 V so that the ratio $r_{sp} = A_{sp}/A_o$ approached 0.1. These tuning parameters were chosen for several reasons. First, they ensure that the phase shift data will be expressed in a predictable manner in the micrographs we collect: dark regions (low phase shift) are softer, while lighter regions (greater phase shift) are harder. Second, these tuning conditions ensure that high phase contrast images will appear, if the mechanical properties of the sample domains are appropriate, i.e., we collect in a "hard-tapping," though intermittent, probe-contact regime (Magonov and Reneker, 1997).

3. Results and discussion

Fig. 1 shows AFM height (A) and phase (B) images of the block face of pure epoxy resin. The height image shows the epoxy to consist of randomly distributed grains and the contrast covers height variations in the 0–3 nm range. The phase image indicates a homogeneous stiffness of these grains.

Fig. 2 shows AFM images of a cross section of a nematode embedded in soft epoxy resin (compare Table 1) in overview (amplitude image, Fig. 2A) and at higher magnification (phase image, Fig. 2B). Fig. 2C shows a TEM image of a similar area of the same nematode.

The comparison of TEM and AFM images indicate that most ultrastructural details from TEM of thin sections can also be visualized by large-scale AFM image of block face. Unlike TEM, no additional treatment for contrast enhancement like heavy metal staining is required. As we will show, however, the contrast in AFM images largely depends on the interaction of the biological material with the embedding resin. Consequently the two microscopies give complementary rather than identical results.

3.1. Surface topography of the block face

The AFM image of embedded nematodes, in contrast to pure embedding resin shows height variation in the range of several hundred nanometers (data not shown). This big corrugation of the surface is attributed to the following factors: (I) the hardness of the embedding resin;

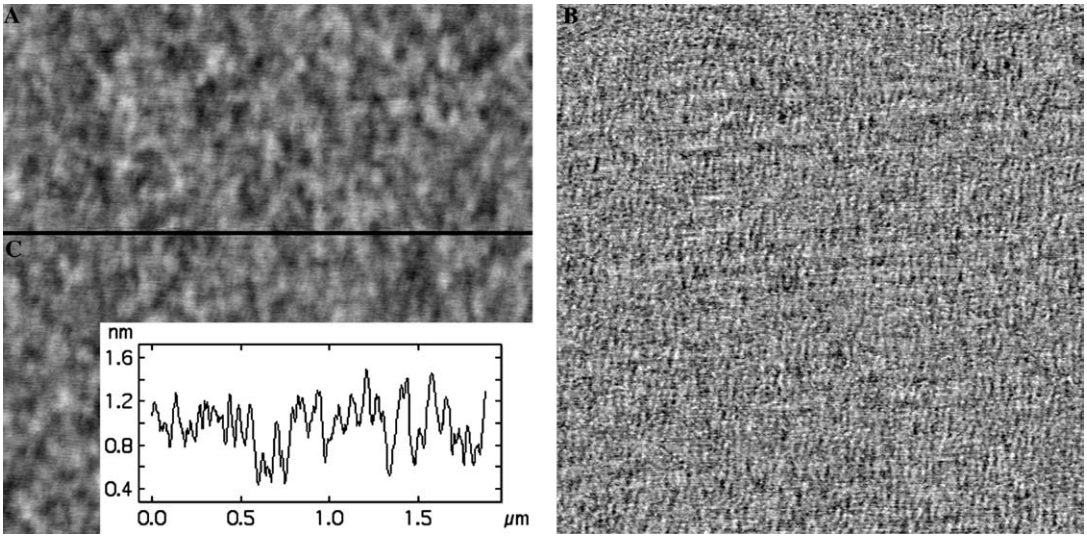

Fig. 1. AFM height (A) and phase (B) images recorded in tapping mode on the block face of the pure epoxy resin after microtomy. The contrast covers height variation of 0–3 nm and phase variation of 0–3°. Graph (C) shows cross-section profile across an arbitrarily selected position in (A). Image width is 2 μm.

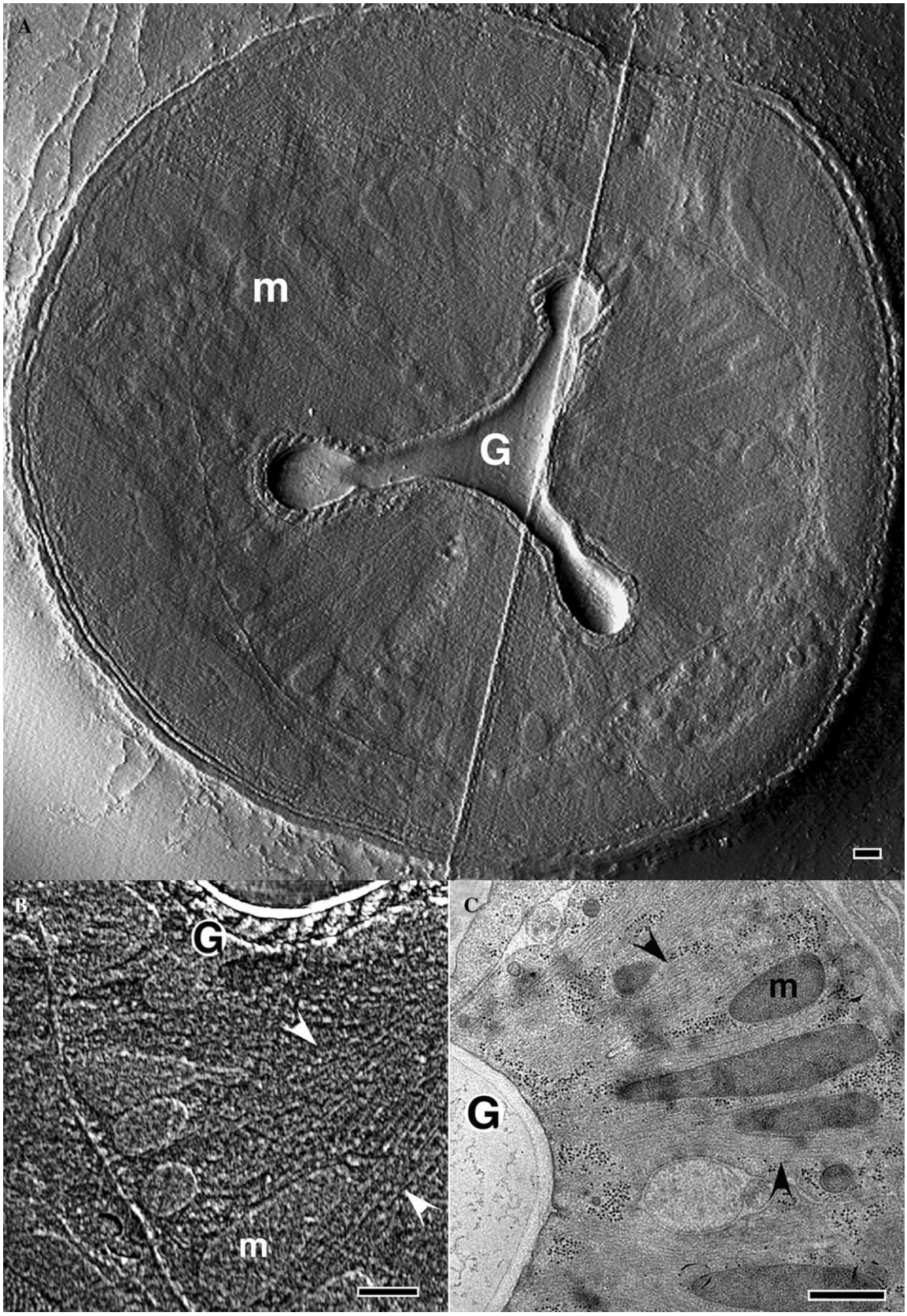

Fig. 2. AFM amplitude (A) and phase (B) images of the block face surface and TEM image (C) of an ultrathin section from the nematode *C. elegans* embedded in soft epoxy resin (Table 1). (B,C) compare AFM and TEM images of a similar area of the same nematode. Amplitude variation, 0–50 nm; phase variation, 0–5°. Scale bars equal 500 nm. Arrows point to actin filaments, **m**, mitochondria; **G**, gut.

(II) the interaction of the resin with the biological structures, and (III) the cleaning of the block-face with ethanol.

Epoxy resins are most frequently used in electron microscopy. In a non-cross-linked stage, the polymer chains are quite distant from each other. When cross-linking agents, e.g., DDSA (or an amine such as DMP-30, which can also crosslink the resins by catalytic mechanism or by bridging) are added, cross bridges are formed resulting in a 3D network structure, which brings the polymer chains close to each other. Due to cross-linking, linear shrinkage of 2% or more is observed in epoxy polymers (Brydson, 1999; Hayat, 2000; Potter, 1970), which probably exerts pressure on the embedded biopolymers.

When biopolymers are impregnated with non-cross-linked epoxy resin, polymer chains which have penetrated inside the specimen can not be cross-linked as tight as in pure plastic by the addition of cross-linker, because of the natural barrier formed by proteins, nucleic acids, lipids etc. This could result in additional tensions, which might squeeze the biopolymers. When the knife, during the sectioning process hits squeezed biopolymers, these may relax and produce topography (compare Fig. 4). Consequently, topography would depend on the hardness of the resin, i.e., on the amount of cross-bridges.

3.2. Dependence of the surface topography on the hardness of the plastic

The hardness of the plastic depends on the quality of polymerization, which on one hand is influenced by the amount of plasticizer present, and on the other hand by the amount of accelerator. While the plasticizer (dibutylphtalate, DP) intercalates between the epoxy chains and prevents the formation of cross-bridges (Lutz and Grossman, 2001), the concentration of the accelerator (2,4,6-tris(dimethylaminomethyl) phenol, DMP-30) determines the velocity of cross-linking, i.e., the time after which the maximum degree of cross-linking is attained (Brydson, 1999).

A number of specimens were prepared using resin formulations with different amount of plasticizer (Table 1).

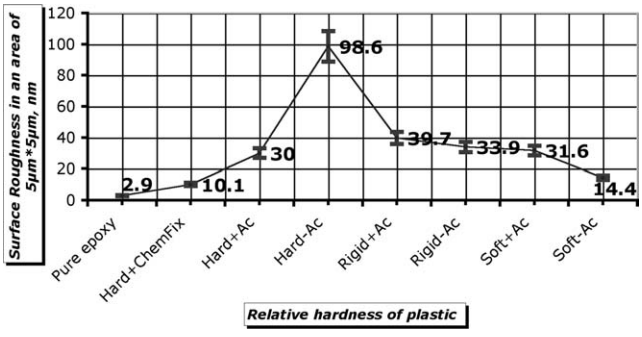

Fig. 3. Graph of the surface roughness of embedded biopolymer depending on the relative hardness of the plastic. For the measurements an area of $5 \times 5\,\mu m$ from longitudinal sections of the gut of *C. elegans* with comparable ultrastructure was selected.

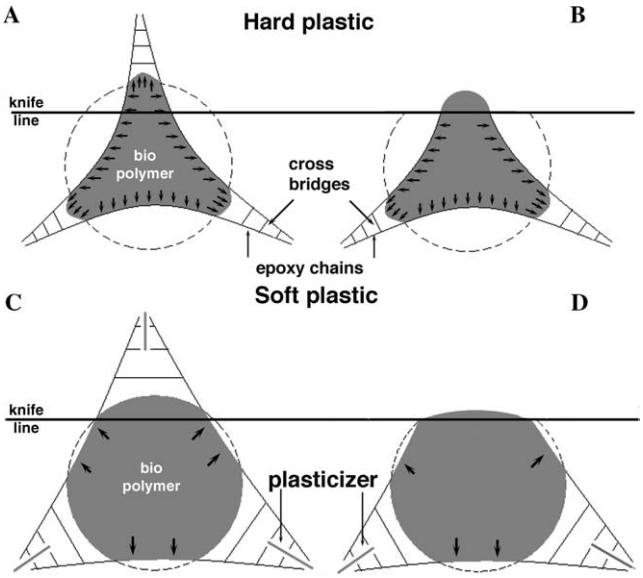

Fig. 4. Scheme of a biopolymer (dashed circle) embedded in hard (A, B) and soft (C, D) epoxy resin. When the embedded biopolymer is sectioned, it tries to relax in the direction of the arrows.

For each resin formulation, embedding was performed with and without accelerator in the first two steps of the embedding procedure (see Section 2) to reach a wider range of hardness of the plastic.

Fig. 3 summarizes surface roughness of the block face of embedded nematodes versus the relative hardness of the plastic. The graph indicates that the highest topographical contrast was detected on the specimen embedded in hard plastic, without plasticizer, and without accelerator in the first two steps of embedding. It thus was not completely cross-linked. On one side the topographic contrast diminished with increasing hardness of the resin (Figs. 4A and B). On the other side, the softest plastic also showed very small height contrast.

The reason might be, that the polymer chains which were separated from each other by plasticizer molecules had fewer cross-bridges, and consequently did not sufficiently squeeze the biopolymers, so that after sectioning almost no relaxation of the structures took place to produce topographical contrast (Figs. 4C and D).

Biological material chemically fixed by glutaraldehyde and osmiumtetroxide showed low (1–10 nm) topographic contrast. We assume that the fixed biological material represents itself a polymer network which, infiltrated by the embedding resin produces a much denser copolymer-network between resin and biopolymers (Causton, 1985). Biopolymers therefore can no longer relax upon sectioning.

3.3. Detectability of small structural details

Fig. 5 compares AFM height and phase images of the gut region of the nematode *C. elegans*, embedded in soft (A–C), rigid (D–F) and hard (G–I) plastic after 7 min

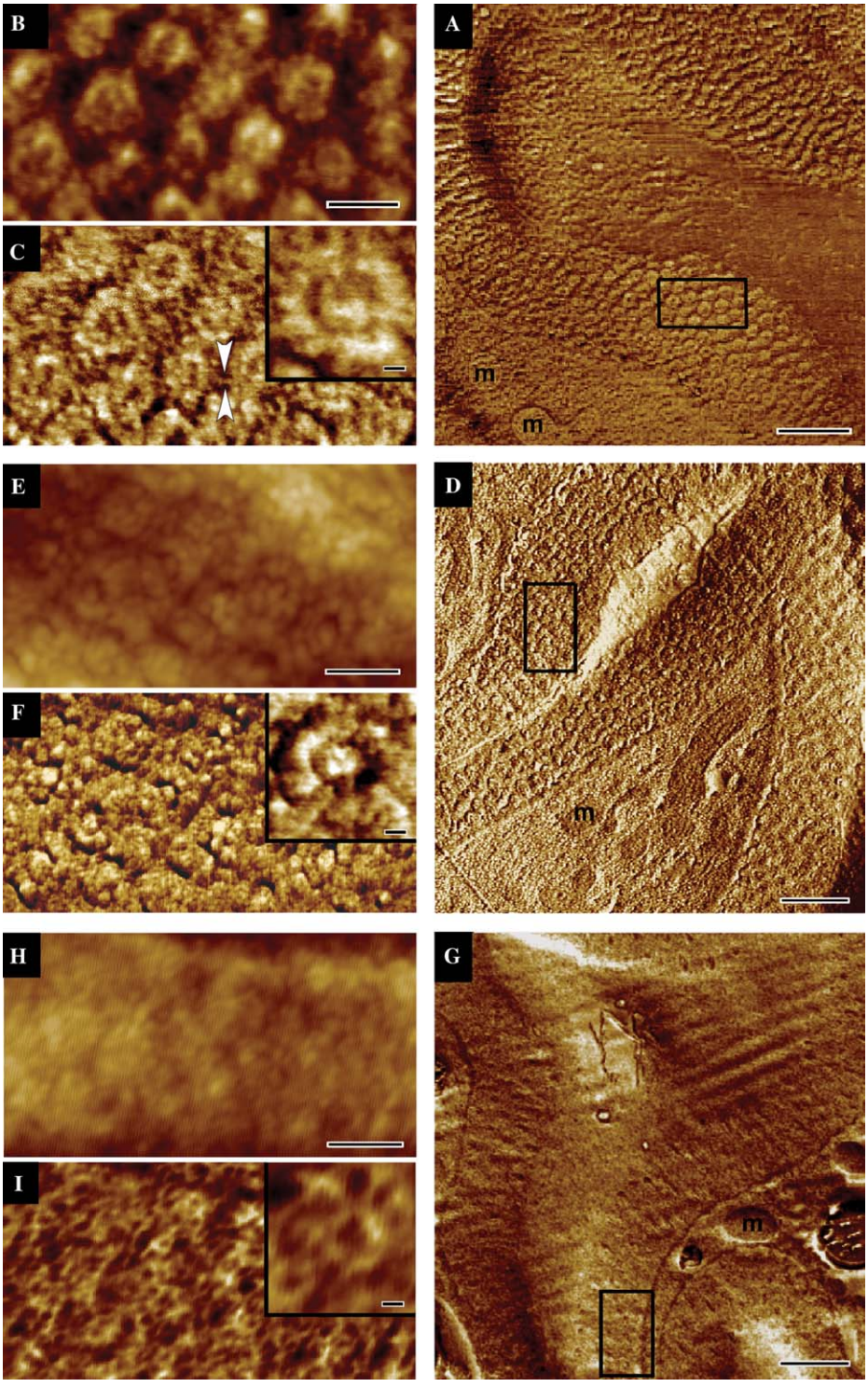

Fig. 5. AFM height (B, E, and H) and phase (A, C, D, F, G, and I) images of the gut region of the nematode C. elegans, embedded in soft (A–C), rigid (D–F), and hard (G–I) plastic. (A, D, and G) show overviews of longitudinal sections of the gut, and (B, C, E, F, H, and I) show cross sectioned microvilli of the gut at higher magnification. The contrast covers height variation in the 0–10 nm in (B, E, and H) and phase variations of 0–5° in (C, F), of 0–10° in (A, D), of 0–20° in (I) and of 0–30° in (G). White arrows (C) indicate a small filament of the glycocalix. Scale bars correspond to 1 μm in (A, D, and G) and 200 nm in (B, C, E, F, H, and I). The scale bar of the magnifier images of the microvilli equals 25 nm.

treatment with Ethanol (see below). (Figs. A, D, and G: overview phase images, and B, C, E, F, H, and I: height and phase images of cross-sectioned microvilli at higher magnification).

Microvilli are small finger-like structures of the cell membrane that protrude into the lumen of the gut (Fig. 6). Bundels of actinfilaments (white arrows) are detected in the center of the microvilli. The microvilli are

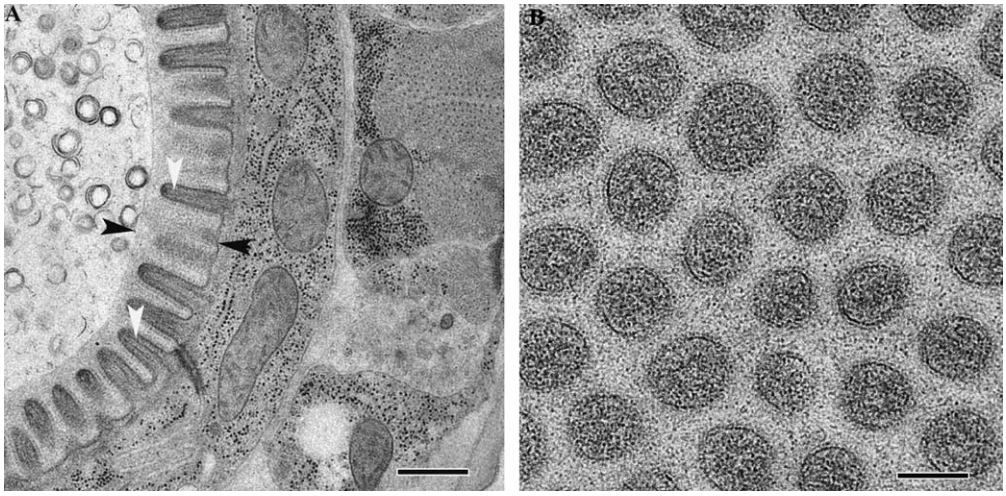

Fig. 6. TEM images of the gut region (A) and of crossectioned microvilli at higher magnification (B) of the nematode *C. elegans*, embedded in soft epoxy. White arrows indicate bundles of actin filaments. Black arrows indicate glycocalix. Scale bars correspond to 1 μm in (A) and 100 nm in (B).

embedded in a glycocalix (Fig. 6 black arrows) which consists of small filaments (Coluccio, 1997; Lange and Gartzke, 2001).

AFM height and phase images reveal bundles of actin filaments inside the microvilli surrounded by a membrane. Due to the epoxy resin-protein interaction, membranes seem to be outlined by the detection of their proteins. The detectability of small structural details is different for specimens embedded in soft, hard, and rigid plastic. While even small filaments in the glycocalix are seen in the soft specimen, it is difficult to observe each individual microvillus in the hard plastic. It is important to note that the phase image of specimens embedded in hard plastic indicates that the biological components are softer (dark signal) than the surrounding plastic (white signal). In hard plastic the polymer chains create a very tough net around the structural elements (organelles, membranes, and macromolecules), but due to high viscosity the resin cannot really penetrate into them. Upon polymerization, a very high tension from outside to inside of the structural element could result (see Fig. 4). If the tension is too high, structural elements might be distorted, because they are kept in unnaturally close proximity to resin molecules with which they are incompatible. This could be the reason, why the structural preservation is reduced in specimens embedded in hard epoxy formulations as known from TEM investigations (Mollenhauer, 1964).

Softer specimen show better structural preservation. Suitable ultrathin sections of very soft epoxy resin, however, are difficult to obtain and it is much easier to get an undistorted block face for AFM examination.

3.4. Ethanol cleaning of the block face

Our results indicate that the best detection of small structural details is achieved by AFM when we can remove a maximum of material from the vicinity of a firmly embedded and copolymerized object.

Treatment with ethanol can elutriate free polymer chains which are not involved in the polymer network and excess of crosslinker which did not react with epoxy chains thereby producing a defined corrugation of the surface of section and block, respectively. Ethanol cannot dissolve tissue components which are stabilized by epoxy resin, but can dissolve an incompletely polymerized polymer network. Ethanol treatment appears to produce more surface corrugation, if the maximum degree of cross-linking (this may take weeks) is not yet attained. This is also illustrated by Fig. 5 where the effect of the ethanol treatment gradually decreases from soft to hard.

Fig. 7 shows height and phase images of *C. elegans* embedded in our softest epoxy formulation before (A and C) and after (B and D) ethanol treatment. After a 15 min exposure to ethanol we can distinguish mitochondria (**m**), actin filaments (black arrows), and many white granular structures which presumably represent proteins (compare also Section 2 and Fig. 8, where the ribosomes appear as white grains).

3.5. Phase contrast reflects the interaction of resin with biological material

The interaction of embedding resins with biological material is very complex. Some aspects of tissue infiltration have been addressed by Mollenhauer and Drolesky (1997). The viscosity of the various components of the resin formulation determines the quality of impregnation of the different biological structures and may result in local variations of the initial resin formulation depending on the permeability (porosity) of the cellular constituents. These local variations of the resin formulation may additionally be influenced by the interaction of the highly reactive epoxy-group with

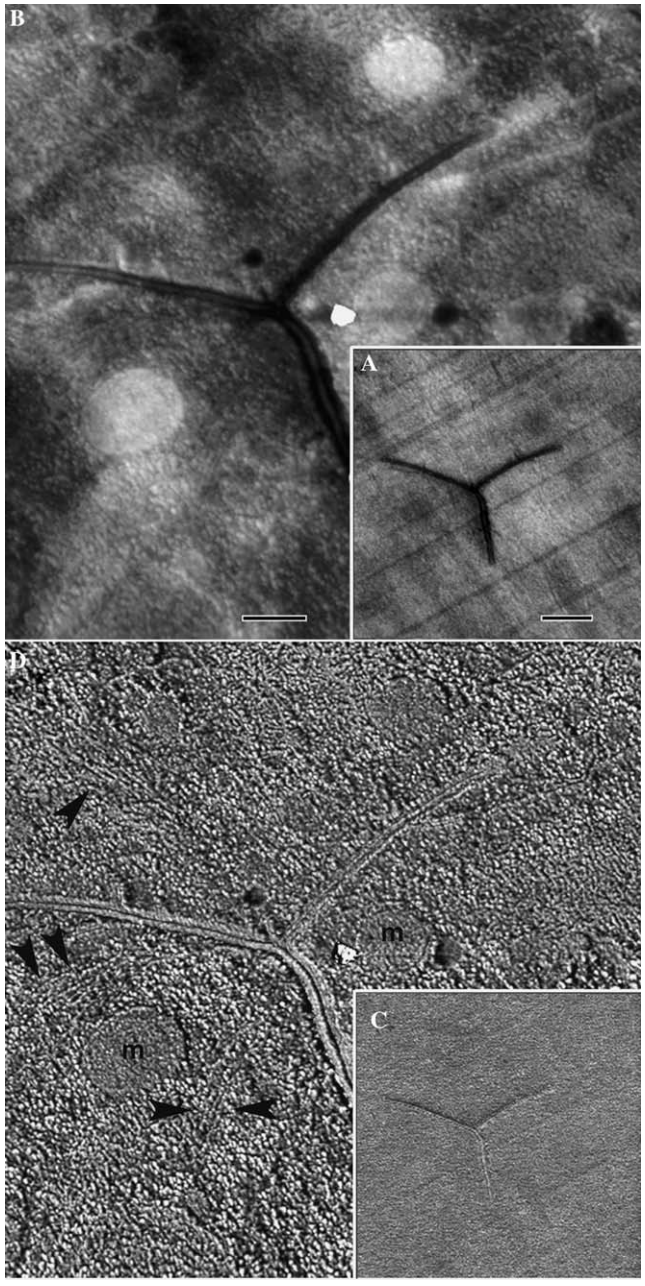

Fig. 7. AFM height (A, B) and phase (D, C) images of *C. elegans* embedded in softest epoxy formulation before (A, C) and after ethanol treatment (B, D) (see Section 2). The contrast covers height variation of 0–20 nm in (A) and of 0–50 nm in (B). The phase varies in the 0–2° range in (C) and in the 0–5° range in (D). Black arrows indicate actin filaments, **m**, mitochondria. Scale bar equals 500 nm.

the biological material (free amino and carboxy-groups of proteins Causton, 1985). Thus, the resin embedded and polymerized biological material will have a locally variable hardness and a locally variable amount of non-cross-linked resin and other molecules of the embedding cocktail which—after removal by ethanol—may reflect the spatial distribution of the biological constituents.

The different interaction of the biological constituents with the embedding resin in AFM is best visualized by phase contrast using a hard tapping mode which reflects the stiffness variation of the examined surface.

3.6. Structural information of the resin embedded biological materials obtained by TEM and AFM

The experimental setup described above, permits the simultaneous examination of the block face by AFM and the corresponding thin section by transmission electron microscopy. In TEM, the ultrastructure is visualized by staining with heavy metals, but only the structures which react with the staining agents and which can be reached by the staining agents are detected. In addition the 2D TEM image represents a projection (superposition) of all sufficiently scattering structures from 50 to 90 nm thick volume. Consequently, cell organelles, membranes, protein filaments, and nucleic acids are clearly detected but e.g., many proteins in the cytoplasm of the cell are practically invisible (Hayat, 2000).

AFM on the contrary, images the very surface of the cut block. Instead of heavy metal stained structures it uses height and/or stiffness variations which depend on the interaction of the epoxy resin with the ultrastructural components. We, therefore, cannot expect that AFM provides structural information identical to TEM but similar and showing new ultrastructural aspects.

Fig. 8A, B, and D shows AFM height and phase blockface images of a section through an epoxy embedded nematode. Fig. 8C presents a TEM image of a section of a similar area from the same block. In both images one can observe mitochondria delineated by membranes, the two membranes of the nuclear envelope and the endoplasmatic reticulum (ER). In the AFM phase image the membranes are detected as a chain of bright grains which may represent the membrane proteins. This assumption is supported by the appearance of the ER which is delineated by the ribosomes and of the nuclear envelope of which the inner membrane seems to consist of more or bigger proteins than the outer membrane (Fig. 8D) The bright grains in the cytoplasm and the nuclear matrix seem to have nearly the same hardness as the membrane grains. They therefore, could represent individual protein molecules.

In conclusion, AFM proves to be an exciting tool to extract ultrastructural information from the interior of cells and tissues. Our initial data suggest a resolution at, or close to the molecular level and the information to be complementary to TEM of thin sections. With evolving sample preparation and because of the nature of the scanning probe techniques, we may soon be able to address the cellular and molecular structures individually, revealing receptor–ligand binding or observing fluorescent labels (using a scanning near-filed optical microscope) at surpassing resolution to name two examples.

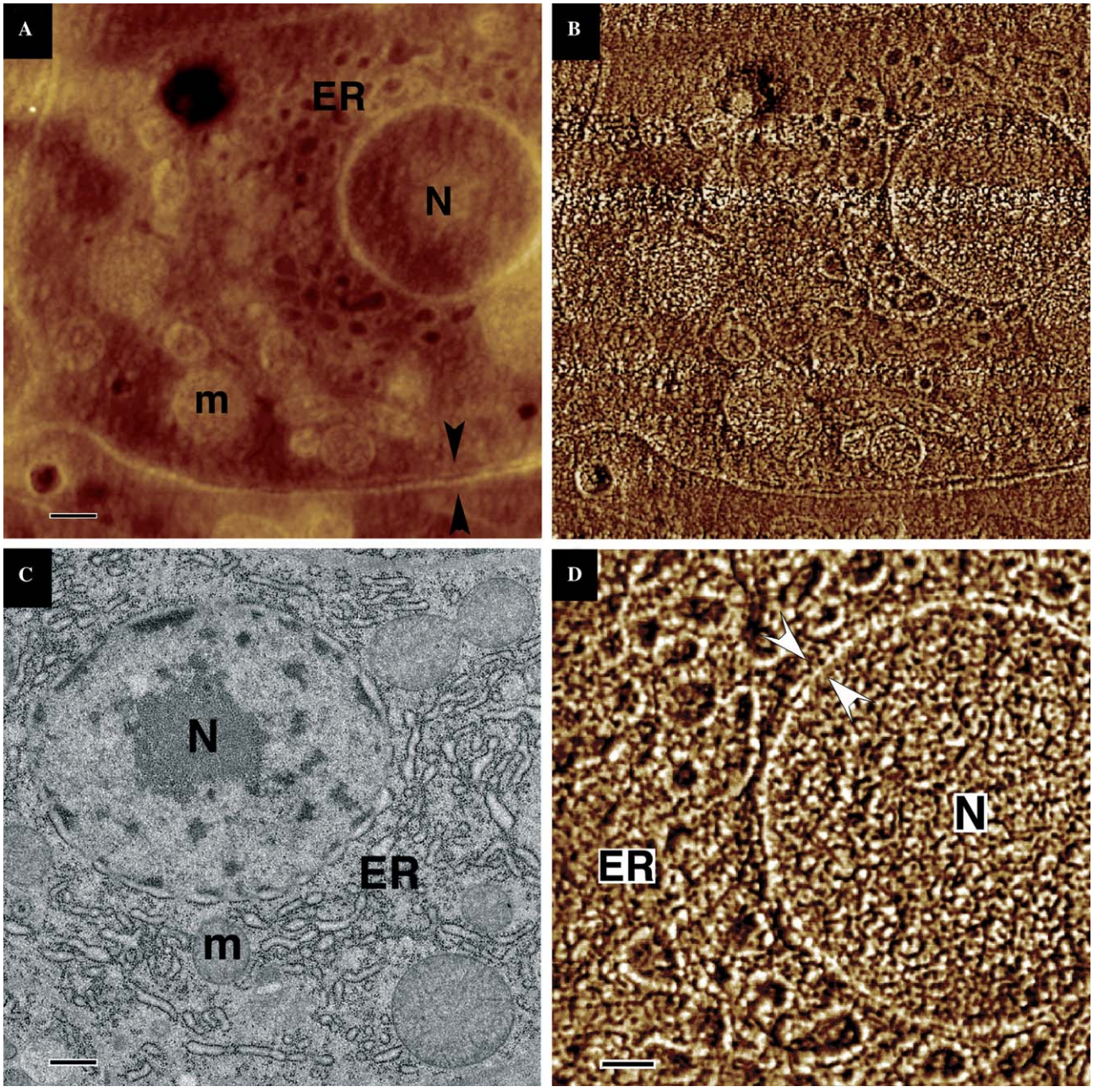

Fig. 8. AFM height (A), phase (B, D) images and TEM (C) image of the cross section of the cell from the epoxy embedded nematode. The contrast covers height variation of 0–100 nm in (A) and phase variation in the 0–5° range in (B, C). Scale bars correspond to 500 nm in (A, B, and C) and 50 nm in (D). White arrows indicate double membrane of the nuclear envelope. Black arrows indicate cell membrane. **N**, nucleus; **ER**, endoplasmic reticulum; and **m**, mitochondria.

Acknowledgments

We thank Monica Gotta for the generous supply of *C. elegans*. We are very grateful to Andreas Stemmer and collaborators for the permission to use their AFM and for stimulating discussion. We are equally indebted to Vikas Mittal for his help in understanding the curing phenomena of epoxy, and to Matthias Amrein for help with the manuscript.

References

Abraham, F.F., Batra, I.P., Ciraci, S., 1988. Effect of tip profile on atomic-force microscope images: a model study. Phys. Rev. Lett. 60, 1314–1317.

Akamine, S., Barret, R.C., Quate, C.F., 1990. Improved atomic force microscope images using microcantilevers with sharp tips. Appl. Phys. Lett. 57, 316–318.

Brydson, J.A., 1999. Plastics Materials, seventh ed. Butterworth–Heinemann, Oxford.

Causton, B.E., 1985. Does the embedding chemistry interact with tissue? In: Mueller, M., Becker, R.P., Boyde, A., Wolosewick, J.J. (Eds.), The Science of Biological Specimen Preparation for Microscopy and Microanalysis. Scanning Electron Microscopy inc., AMF O'Hare, pp. 209–214.

Coluccio, L.M., 1997. Myosin I. Am. J. Physiol. 273, 347–359.

Dahl, R., Staehelin, L.A., 1989. High pressure freezing for the preservation of biological structure: theory and practice. J. Electron Microsc. Techn. 13, 165–174.

Fasolka, M.J., Mayes, A.M., Magonov, S.N., 2001. Thermal enhancement of AFM phase contrast for imaging diblock copolymer thin film morphology. Ultramicroscopy 90, 21–31.

Haugstad, G., Jones, R., 1999. Mechanisms of dynamic force microscopy on polyvinyl alcohol: region-specific non-contact and intermittent contact regimes. Ultramicroscopy 76, 77–86.

Hayat, M.A., 2000. Principles and Techniques of Electron Microscopy: Biological Applications, fourth ed. Cambridge University Press, Cambridge.

Hohenberg, H., Mannweiler, K., Mueller, M., 1994. High-pressure freezing of cell suspensions in cellulose capillary tubes. J. Microsc. (Oxford) 175 (1), 34–43.

Jesior, J.-C., 1985. How to avoid compression: a model study of latex sphere grid sections. J. Ultrastruct. Res. 90, 135–144.

Jesior, J.-C., 1986. How to avoid compression: II. The influence of sectioning conditions. J. Ultrastruct. Mol. Res. 95, 210–217.

Lange, K., Gartzke, J., 2001. Microvillar cell surface as a natural defense system against xenobiotics: a new interpretation of multidrug resistance. Am. J. Physiol. Cell Physiol. 281 (2), 369–385.

Luft, J.H., 1961. Improvements in epoxy resin embedding methods. J. Biophys. Biochem. Cytol. 9, 409–414.

Lutz, J.T., Grossman, R.F., 2001. Polymer Modifiers and Additives. Marcel Dekker, NY.

Magonov, S., Reneker, D., 1997. Characterization of polymer surfaces with atomic force microscopy. Annu. Rev. Mater. Sci. 27, 175–222.

Melling, M., Hochmeister, S., Blumer, R., Schilcher, K., Mostler, S., Behnam, M., Wilde, J., Karimian-Teherani, D., 2001. Atomic force microscopy imaging of the human trigeminal ganglion. Neuroimage 14 (6), 1348–1352.

Menco, B.P., 1984. Ciliated and microvillous structures of rat olfactory and nasal respiratory epithelia. A study using ultra-rapid cryofixation followed by freeze-substitution or freeze-etching. Cell Tissue Res. 235 (2), 225–241.

Menco, B.P., 1995. Freeze-fracture, deep-etch, and freeze-substitution studies of olfactory epithelia, with special emphasis on immunocytochemical variables. Microsc. Res. Tech. 32 (4), 337–356.

Mollenhauer, H.H., 1964. Plastic embedding mixtures for use in electron microscopy. Stain Technol. 39, 111.

Mollenhauer, H.H., Drolesky, R.E., 1997. Image contrast in sections of epoxy resin-embedded biological material: maintenance of a proper anhydride-epoxy ratio during tissue impregnation. Microsc. Res. Technol. 36, 417.

Moor, H., Hochli, M., 1968. Snap freezing under high pressure: a new fixation technique for freeze-etching. In: Favard, P. (Ed.), Proc. Fourth Eur. Reg. Conf. Electr. Microsc. pp. 445–446.

Moor, H., 1987. Theory and practice of high-pressure freezing. In: Steinbrecht, R.A., Zierold, K. (Eds.), Cryo-techniques in Biological Electron Microscopy. Springer-Verlag, Berlin, Heidelberg, pp. 175–191.

Mueller, M., Moor, H., 1984. Cryofixation of thick specimens by high pressure freezing. In: Mueller, M., Becker, R.P., Boyde, A., Wolosewick, J.J. (Eds.), The Science of Biological Specimen Preparation, SEM. AFM O'Hare, Chicago, IL, pp. 131–138.

Nag, K., Munro, J.G., Hearn, S.A., Rasmusson, J., Petersen, N.O., Possmayer, F., 1999. Correlated atomic force and transmission electron microscopy of nanotubular structures in pulmonary surfactant. J. Struct. Biol. 126 (1), 1–15.

Potter, W.G., 1970. Epoxide Resins. Iliffe Books, London.

Studer, D., Henneke, H., Mueller, M., 1992. High pressure freezing of soybean nodules leads to an improved preservation of ultrastructure. Planta 188, 155–163.

Van Harreveld, A., Crowell, J., 1964. Electron microscopy after rapid freezing on a metal surface and substitution fixation. Anat. Rec. 149, 381–386.

Yamamoto, A., Tashiro, Y., 1994. Visualization by an atomic force microscope of the surface of ultra-thin sections of rat kidney and liver cells embedded in LR white. J. Histochem. Cytochem. 42 (11), 1463–1470.